



SDC-Carbonate Composite Electrolytes for Low-Temperature SOFCs

Jianbing Huang, Zongqiang Mao,^z Lizhai Yang, and Ranran Peng

Institute of Nuclear and New Energy Technology, Tsinghua University, 100084, Beijing, China

Novel composite materials based on mixtures of samarium-doped ceria (SDC)-carbonate were examined for use as electrolyte materials in low-temperature solid oxide fuel cells (LTSOFCs) operating at 400–600°C. The composite electrolytes showed high ion conductivity at evaluated temperatures. Composition and calcination temperature were found to affect the morphology and conductivity of the composite electrolytes greatly. During fuel cell operation, water was observed at both electrodes, indicating that the new electrolyte materials conduct both oxygen ions and proton simultaneously. According to fuel cell performance, these composite electrolytes are chemically stable, which is an attractive prospect in LTSOFC applications.
© 2005 The Electrochemical Society. [DOI: 10.1149/1.1960139] All rights reserved.

Manuscript submitted January 8, 2005; revised manuscript received April 21, 2005. Available electronically July 18, 2005.

Low-temperature solid oxide fuel cells (LTSOFCs) have received much attention in recent years because they may dramatically contribute to the reduction in the cost of SOFC technology, in which inexpensive materials can be used in cell construction and novel fabrication techniques can be applied to the stack and system integrations due to the low operating temperature. Moreover, the system reliability, life span, and potential applications of SOFC system increase. However, conventional yttrium-stabilized zirconia (YSZ) electrolyte cannot meet demands of low-temperature operation even using thin-film technology.¹ It is therefore vital to develop new electrolyte materials that can provide high ion conductivities at low temperature for advanced LTSOFCs.

Doped ceria and lanthanum gallate are being widely investigated as the potential electrolyte materials for LTSOFCs due to their high oxygen ion conductivities.^{2,3} Whereas, doped ceria (DCO) can cause a certain electronic conduction in the reduced fuel environment and result in lower open-circuit voltage and less power output. For doped lanthanum gallate, it is quite difficult to find suitable electrodes.

Recently, a new type of electrolyte materials known as ceria-salt composites (CSC) has been developed for the application of LTSOFCs.^{4–9} The CSC could effectively suppress the electronic conduction of DCO and enhance significantly ionic conductivities. These composite materials were found to conduct both oxygen ion and proton during the fuel cell environment, thus result in high LTSOFC performance.

Until now, most studies of the composite electrolytes were focused on the performance of the fuel cells with the composite electrolytes, while the materials were seldom investigated. In this paper, the structure, morphology, and electrical property of one type of the CSC electrolytes, SDC- Li_2CO_3 - K_2CO_3 , was studied, and the properties of fuel cell assemblies with the SDC- Li_2CO_3 - K_2CO_3 electrolyte were investigated.

Experimental

Preparation of SDC-carbonate composite electrolyte.—The powders of samarium-doped ceria (SDC, $\text{Ce}_{0.8}\text{Sm}_{0.2}\text{O}_{1.9}$) were synthesized as described in Ref. 10. Li_2CO_3 and K_2CO_3 were mixed in the mol ratio of 62:38, and heated at 500°C in air for 1 h to form an eutectic salt. The eutectic salt and SDC were mixed in various weight ratios (15, 20, 30, and 45%), ground thoroughly in an agate mortar, calcined at various temperatures (500, 600, 700, and 800°C) in air for 1 h, to obtain SDC-carbonate composite.

Characterization of composite electrolyte.—The calcined composite electrolyte powder was cold pressed at 250 MPa into cylindrical pellets (13 mm diam and ~1 mm thick) using a uniaxial die-press. The green pellets were then sintered at 600°C for 1 h. Silver electrodes were subsequently prepared by painting silver

paste onto either side of the pellets, and heated at 600°C for 40 min. Electrical conductivity of the pellet samples was then measured in air by ac impedance spectroscopy at the temperature between 400 and 650°C. The measurements were conducted using a PerkinElmer 5210 frequency response analyzer (0.5 Hz to 120 KHz) combined with EG&G PAR potentiostat/galvanostat 263A.

The powder X-ray diffraction (XRD) patterns of the composite electrolytes were recorded at room temperature using a D8 diffractometer (Bruker Corp. Germany) that employs $\text{CuK}\alpha$ radiation. The morphology of powders and the microstructure of sintered pellets were characterized by scanning electron microscopy (SEM, JSM-6301F).

Fuel cell components and construction.—The fuel cells were constructed using a composite anode-supported technique. The composite anode was the mixture of NiO (50 vol %) and electrolyte (50 vol %). The cathode powder was composed of lithiated NiO (50 vol %) mixed with electrolyte (50 vol %). The anode, electrolyte and cathode were uniaxially pressed into a pellet at a pressure of 250 MPa and then sintered at 600°C for 30 min in air. The cell size was 13 mm in diam and 1–2 mm thick. Silver paste was coated afterwards on cathode surface to act as current collector.

Homemade apparatus were used for the performance measurement of the fuel cell assemblies. The fuel cells were tested between 400 and 600°C. Hydrogen and air were used as the fuel and the oxidant, respectively. The gas flow rates were controlled between 60–90 mL/min under 1 atm pressures.

Results and Discussion

Phase and microstructures of composite electrolyte.—Figure 1 shows the powder XRD patterns of pure SDC and SDC- Li_2CO_3 - K_2CO_3 composite electrolytes with various salt contents at room temperature. All the composite samples show the same diffractions that were identified for SDC phase, indicating that the carbonates exist as an amorphous phase after thorough grinding and heat-treatment. It is assumed that the carbonates can be melted and be coated on the SDC particles during the heat-treatment.

The morphology of the composites with various salt contents after calcined at 600°C is shown in Fig. 2, which shows that the composition affects the morphology of the composite obviously. For pure SDC powder, the particles possess pillar structure. But for the composites, the morphology becomes amorphous due to SDC particles covered with carbonates.

Figure 3 presents the micrographs of the SDC-30 wt % (62 mol % Li_2CO_3 -38 mol % K_2CO_3) composite powders calcined at different temperatures. It is shown that all samples agglomerate together to form a homogenous bulk. With the calcination temperature increases, the composites become homogenous and the interface between SDC particles and carbonates forms. This interface has much to do with the continuous ion-conducting path.

The surface morphologies of the SDC-(62 mol % Li_2CO_3 -38 mol % K_2CO_3) composite pellets sintered at 600°C with

^z E-mail: maozq@tsinghua.edu.cn

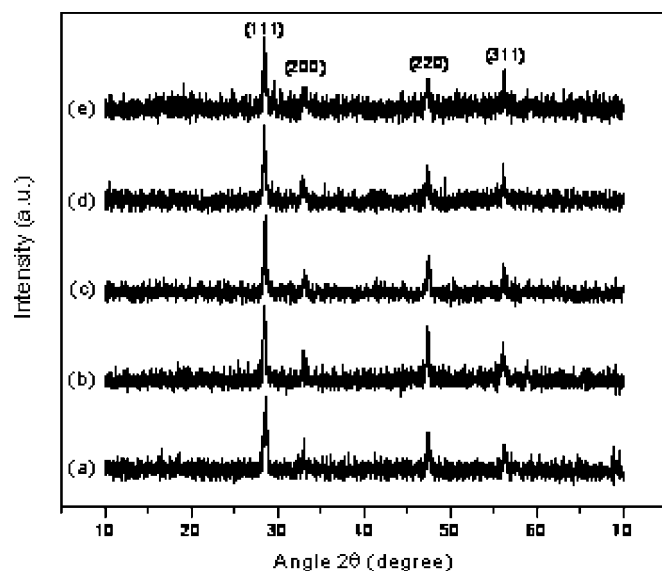


Figure 1. XRD patterns for (a) SDC and SDC-(62 mol % $\text{Li}_2\text{CO}_3\text{-K}_2\text{CO}_3$) composites with salt contents of (b) 15, (c) 20, (d) 30, and (e) 45 wt %.

different salt content are shown in Fig. 4. From the SEM images, significant changes in the particle topography can be seen. As the salt content increases, more salts cover the SDC particles leading to a smooth surface. However, when the salt content reaches to 45 wt %, obvious acicular crystals are observed on the surface of the composite pellet. This indicates a composition limit of the salt to form a good SDC-carbonate composite, but it is necessary to investigate further the salt content between 30 and 45 wt %.

Electrical conductivities of composite electrolyte.—The conductivities of SDC-(62 mol % $\text{Li}_2\text{CO}_3\text{-38 mol % K}_2\text{CO}_3$) composite electrolytes with various salt contents obtained from ac impedance analysis are shown in Fig. 5. A sharp discontinuity is seen in the $\ln(\sigma T)$ vs. $1/T$ plot. The discontinuity can be interpreted as a superionic phase transition in the boundary phase formed between the constituent phases. It is well known that the addition of a second phase (such as Al_2O_3 , SiO_2 , and CeO_2) into the salt phase can enhance the conductivity of the materials.¹¹ The conductivity enhance-

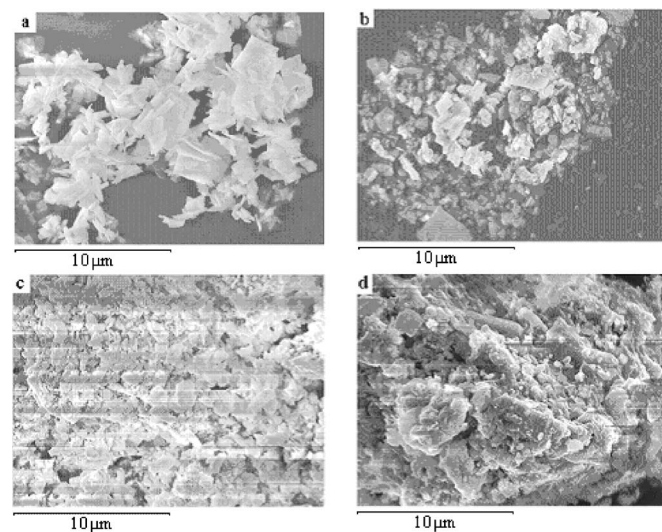


Figure 2. SEM images of (a) the pure SDC and SDC-(62 mol % $\text{Li}_2\text{CO}_3\text{-K}_2\text{CO}_3$) composites with salt contents of (b) 20, (c) 30, and (d) 45 wt %.

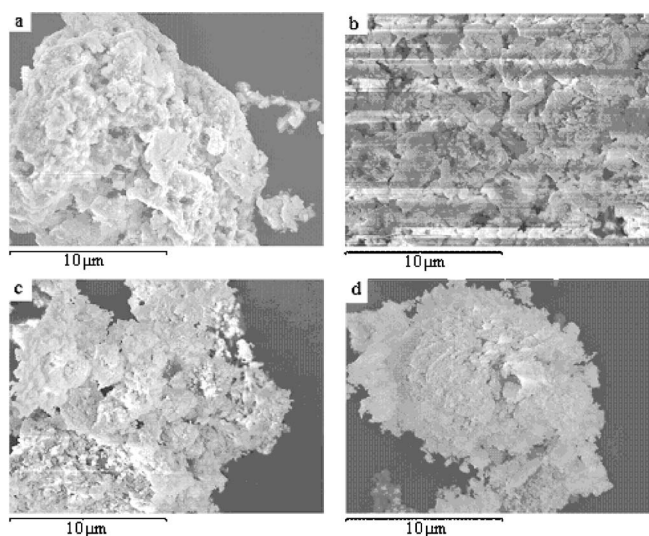


Figure 3. SEM images of the SDC 30 wt % (62 mol % $\text{Li}_2\text{CO}_3\text{-K}_2\text{CO}_3$) composite powders calcined at (a) 500 (b) 600, (c) 700, and (d) 800°C.

ment is assumed to be the effect of the second phase on the space charge zones near phase boundaries.¹² The conductivity enhancement of SDC-carbonate composite can also be explained in a similar way. However, the SDC phase is an oxygen ion conducting phase, not an insulated phase, and the space charge zones of the two phases may interact leading to an enhanced conductivity.

As shown in Fig. 5, the discontinuity occurs at different temperature with different salt content, e.g., the transition temperature of the composite with salt content of 15, 20, and 30 wt % is 450, 450, and 475°C, respectively. As we know, the melting point of Li_2CO_3 and K_2CO_3 is 618 and 850°C, respectively. And the melting point of 62 mol % $\text{Li}_2\text{CO}_3\text{-38 mol % K}_2\text{CO}_3$ eutectic salt is 490°C. It is evident that the melting point of the salts is higher than the transition temperatures, indicating that the enhanced conductivity does not result from the molten carbonates, but from the superionic interface phase. However, when the salt content reach to 45%, the composite effect becomes worse due to the excess salt to the composition limit, which identified by the SEM. Although the conductivity of the composite with 45% salt above the transition temperature is higher than

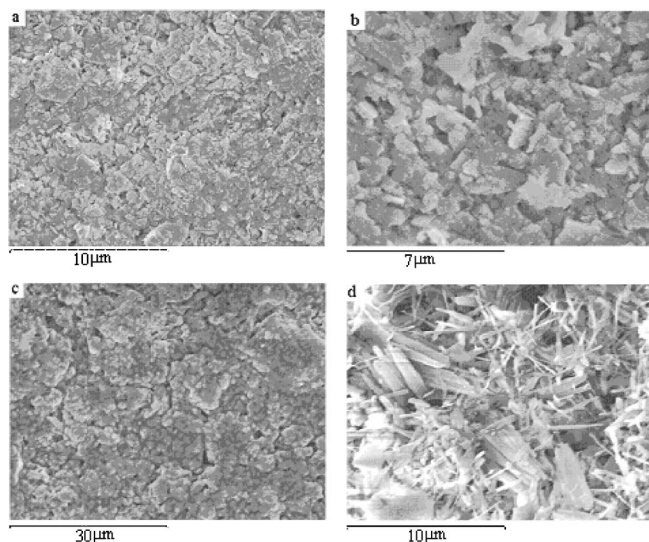


Figure 4. Surface SEM images of the SDC-(62 mol % $\text{Li}_2\text{CO}_3\text{-K}_2\text{CO}_3$) composite pellets with salt contents of (a) 15 (b) 20, (c) 30, and (d) 45 wt %.

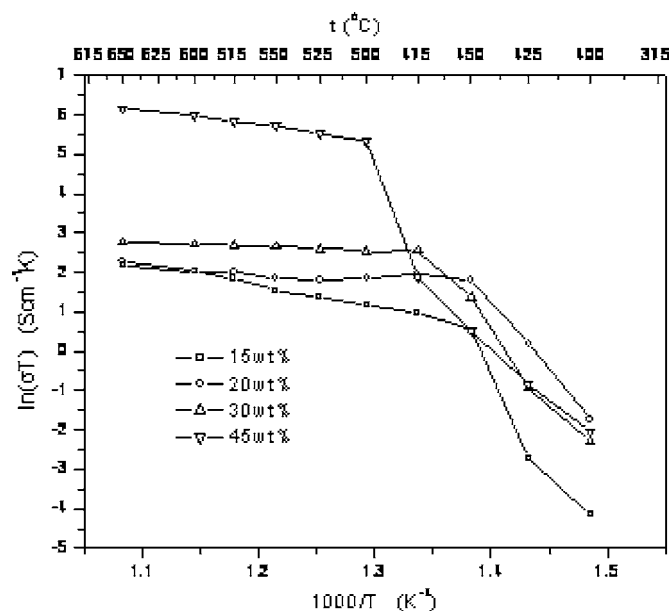


Figure 5. Arrhenius plots of the SDC-(62 mol % $\text{Li}_2\text{CO}_3\text{-K}_2\text{CO}_3$) composite pellets with various salt contents.

that of the samples with less salt content, its high conductivity comes from the molten carbonates, but not from the interface phase, because the transition temperature (500°C) is similar to the melting point of the eutectic carbonates.

Figure 6 presents the Arrhenius plot for the SDC-30 wt % (62 mol % $\text{Li}_2\text{CO}_3\text{-K}_2\text{CO}_3$) composite electrolyte calcined at various temperatures. It is observed that the calcination temperature has an influence on the conductivity. Each curve consists of two lines with the same transition temperature (475°C) except for the composite calcined at 700°C. From the slopes, we can conclude that above the transition temperatures the conducting activation energy of various samples is almost the same. When the composite calcined at 500°C, the composite effect is poor in that the conductivity is much lower than that of the composite calcined at 600, 700, and 800°C. When calcined at above 600°C, the conductivity of the com-

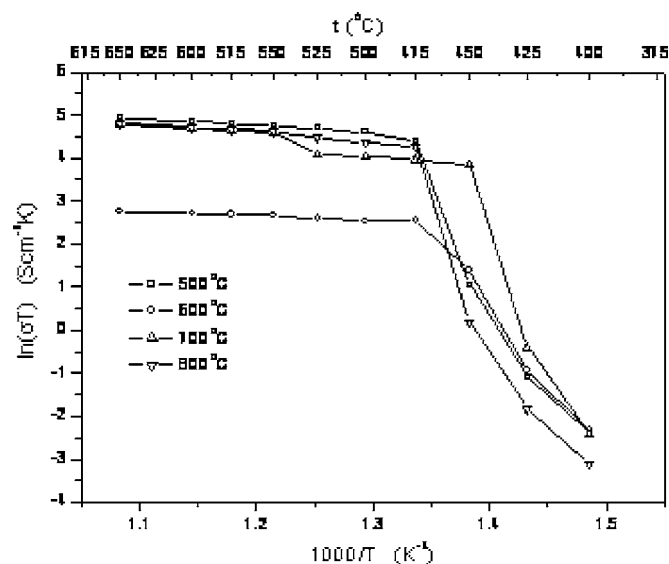


Figure 6. Arrhenius plots of the SDC 30 wt % (62 mol % $\text{Li}_2\text{CO}_3\text{-K}_2\text{CO}_3$) composite electrolyte calcined at various temperatures.

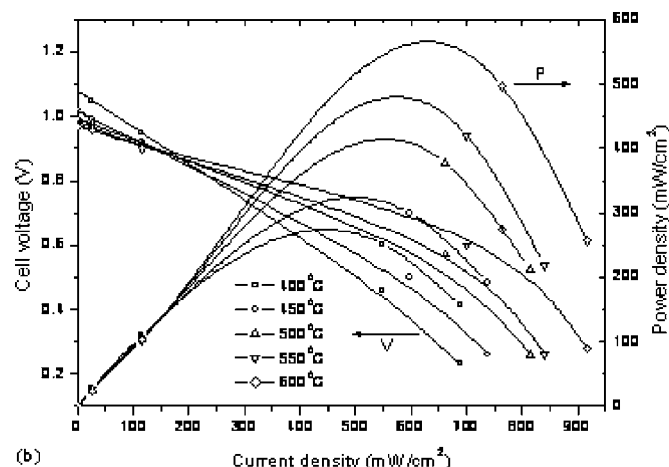


Figure 7. I-V and I-P characteristics for the fuel cell using the SDC 20 wt % (62 mol % $\text{Li}_2\text{CO}_3\text{-K}_2\text{CO}_3$) composite electrolyte at various temperatures.

posite above the transition temperature increases little. Considering the volatilization of carbonate become easier with the increasing calcination temperature, high calcination temperature is not suitable.

It should be emphasized that the conductivity obtained by ac impedance analysis reflects all the transferring ions (including CO_3^{2-} ion, Li^+ and K^+ ions, O^{2-} from SDC) in the bulk material, so the fuel cell I-V characterization is proposed to measure the corresponding conductivities of the composite, yet the conductivity measured by ac impedance is still very useful.

Fuel cell performances.—I-V and I-P characteristics at various temperatures for fuel cell based on the SDC-20 wt % (62 mol % $\text{Li}_2\text{CO}_3\text{-K}_2\text{CO}_3$) composite electrolyte are shown in Fig. 7. The maximum power density of more than 400 and 500 mWcm^{-2} were obtained at 550 and 600°C, respectively. Figure 8 shows the discharging performance for another fuel cell sample with the same electrolyte at 600°C. The cell voltage and current density increase during the initial discharging period within an hour, suggesting that the electrodes were intensively activated and the interfaces between the electrode/electrolyte were improved by discharging. The cell has continuously discharged at a power density of 490 mWcm^{-2} for at least 3 h, implying that the composite electrolyte is chemically stable. And it is expected that the fuel cell performance will be

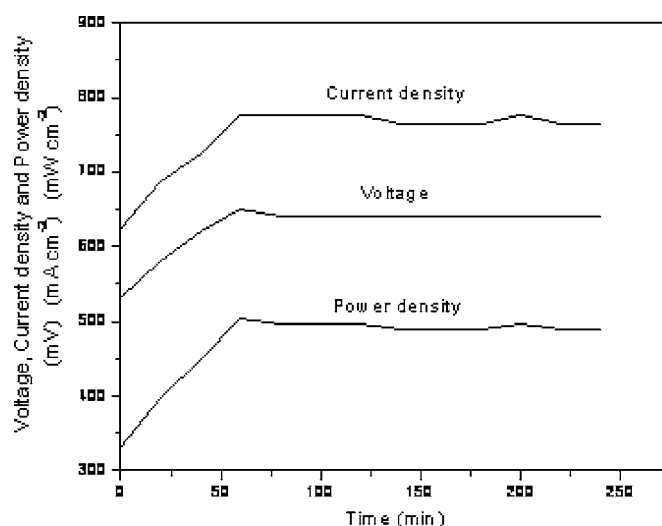


Figure 8. Discharge performance for the fuel cell using the SDC 20 wt % (62 mol % $\text{Li}_2\text{CO}_3\text{-K}_2\text{CO}_3$) composite electrolyte at 600°C.

improved greatly by using compatible electrode materials and additional technical development.

During fuel cell operation, it is observed clearly that water is generated at both the anode and cathode sides, suggesting the existence of both proton and oxygen ion conduction through the composite electrolyte. The hybrid ionic conduction enhances the material conductivity and promotes the electrode reaction kinetics between the electrode/electrolyte interfaces leading to the excellent output performance. Proton conduction may be formed more preferentially at the interfaces between the SDC and carbonates. The carbonate ion CO_3^{2-} can adsorb the proton ionized from hydrogen by catalysis and form transitional state HCO_3^- , which provide one possibility of proton transfer. However, the detailed mechanism of the oxygen ion and proton conduction needs more studies.

Conclusions

New electrolyte materials based on the SDC-carbonate composites were developed and applied for LTSOFC. These new composite materials were a two phase composite ceramic. The morphology and conductivity of the composite electrolytes change greatly with salt content and powder calcination temperature. The results show that the electrical property of the composite is related to the interfaces of composite agglomerating phase and the SDC bulk material. The formation of interface may provide possible paths for proton transport, thus resulting in water produced at both the anode and cathode sides. The fuel cell based on SDC-LiKCO₃ composites electrolyte has demonstrated excellent performance at the low-temperature re-

gion. Compared with pure SDC electrolyte, the SDC-carbonate composite is a more promising electrolyte material for the development of cost-effective and marketable fuel cell technology.

Acknowledgments

This work was supported by China National Hydrogen project (contract no. G2000026410 and 2001AA515080) and by the State Key Laboratory of Automotive Safety and Energy in Tsinghua University.

References

1. R. Maric, S. Seward, P. W. Faguy, and M. Oljaca, *Electrochem. Solid-State Lett.*, **6**, 91 (2003).
2. T. Hibino, A. Hashimoto, T. Inoue, J.-i. Tokuno, S.-i. Yashida, and M. Sano, *Science*, **288**, 2031 (2000).
3. T. Fukui, S. Ohara, K. Murata, H. Yoshida, K. Miura, and T. Inagaki, *J. Power Sources*, **106**, 142 (2002).
4. B. Zhu, X. Liu, and P. Zhou, *J. Mater. Sci. Lett.*, **20**, 591 (2001).
5. B. Zhu, X. Liu, P. Zhou, X. Yang, Z. Zhu, and W. Zhu, *Electrochem. Commun.*, **3**, 566 (2001).
6. B. Zhu, X. T. Yang, J. Xu, Z. G. Zhu, S. J. Ji, M. T. Sun, and J. C. Sun, *J. Power Sources*, **118**, 47 (2003).
7. G. Y. Meng, Q. X. Fu, S. W. Zha, C. R. Xia, X. Q. Liu, and D. K. Peng, *Solid State Ionics*, **148**, 533 (2002).
8. Q. X. Fu, W. Zhang, R. R. Peng, D. K. Peng, G. Y. Meng, and B. Zhu, *Mater. Lett.*, **53**, 186 (2002).
9. B. Zhu, X. Liu, M. Sun, S. Ji, and J. Sun, *Solid State Sci.*, **5**, 1127 (2003).
10. P. Ranran, X. Changrong, P. Dingkun, and M. Guangyao, *Mater. Lett.*, **58**, 604 (2004).
11. C. C. Liang, *J. Electrochem. Soc.*, **120**, 1289 (1973).
12. J. Maier, *Prog. Solid State Chem.*, **23**, 171 (1995).